

# Dispersive stabilization of the inverse cascade for the Kolmogorov flow

B. Legras,<sup>1\*</sup> B. Villone,<sup>2</sup> and U. Frisch<sup>3</sup>

<sup>1</sup> CNRS, LMD/ENS, 24 rue Lhomond, 75231 Paris Cedex 5, France

<sup>2</sup> Istituto di Cosmogeofisica, CNR, C. Fiume 4, 10133 Torino, Italy

<sup>3</sup> CNRS UMR 6529, Observatoire de la Côte d'Azur, BP 4229, 06304 Nice Cedex 4, France

(December 2, 2024)

It is shown by perturbation techniques and numerical simulations that the inverse cascade of kink-antikink annihilations, characteristic of the Kolmogorov flow, is halted by the dispersive action of Rossby waves in the  $\beta$ -plane approximation. For  $\beta \rightarrow 0$ , the largest excited scale is  $\propto \ln 1/\beta$  and differs strongly from what is predicted by standard dimensional phenomenology which ignores depletion of nonlinearity.

PACS number(s): 47.10.+g, 92.60.Ek, 47.27.-i, 47.27.Ak, 47.35.+i

Planetary-scale flow is subject to the competing effects of quasi-two-dimensional turbulence and Rossby waves ( $\beta$ -effect). It is known from phenomenological arguments and numerical simulations that the inverse cascade which characterizes the large-scale dynamics of two-dimensional turbulence in planetary flow can be halted by Rossby wave dispersion and that the ensuing flow exhibits alternating jets. [1–5]. This is an instance of the interaction of waves and turbulence, a subject with a wealth of applications in astro/geophysical flow and plasmas (see, e.g., Ref. [6]).

The case of strongly dispersive waves is reasonably well understood through the theory of resonant wave interactions (Refs. [6,7] and references therein). It is however inapplicable to a rotating planet where the dispersive action of Rossby waves (with a frequency  $\beta/k$ ) is felt only at the very largest scales (small wavenumber  $k$ ). For the case of weakly dispersive waves, the nonlinear dynamics in the absence of waves must be understood before we can find how it is affected by the presence of the waves. Otherwise, we are limited to dimensional arguments such as the balancing of a turnover time and of the wave period as in Ref. [1]. This can be very misleading because it ignores the depletion of nonlinearities which is so common in turbulence [8]. Our present study deals with the Kolmogorov flow [9] for which the inverse cascade is understood rather well in terms of kink-antikink dynamics [10]. The basic Kolmogorov flow is  $\mathbf{u} = (\cos y, 0)$ , obtained by applying to the two-dimensional Navier–Stokes equation a force  $\mathbf{f} = \nu(\cos y, 0)$ . The Kolmogorov flow has a large-scale negative eddy viscosity instability when the kinematic viscosity  $\nu$  is just below the critical value  $\nu_c = 1/\sqrt{2}$  [9]. Close to  $\nu_c$  and in the presence of Rossby waves, the large-scale dynamics is governed by the one-dimensional “ $\beta$ -Cahn–Hilliard” equation with cubic nonlinearity, derived by multiscale techniques in Ref. [7] (see also Ref [11] for the case  $\beta = 0$ ), which reads

$$\partial_t v = \lambda_3 \partial_x^2 U'(v) - \lambda_3 \partial_x^4 v - \beta \partial_x^{-1} v. \quad (1)$$

Here,  $U(v) = s^2(v^4/(2\Gamma^2) - v^2)$  is a quartic potential and  $\partial_x^{-1}$  denotes spatial integration for zero-average functions

in the interval  $[0, L]$  over which periodicity is assumed. (In the original setup of Ref. [7], the constants are  $s = 1/\sqrt{3}$ ,  $\Gamma = \sqrt{3/2}$  and  $\lambda_3 = 3/\sqrt{2}$ .)

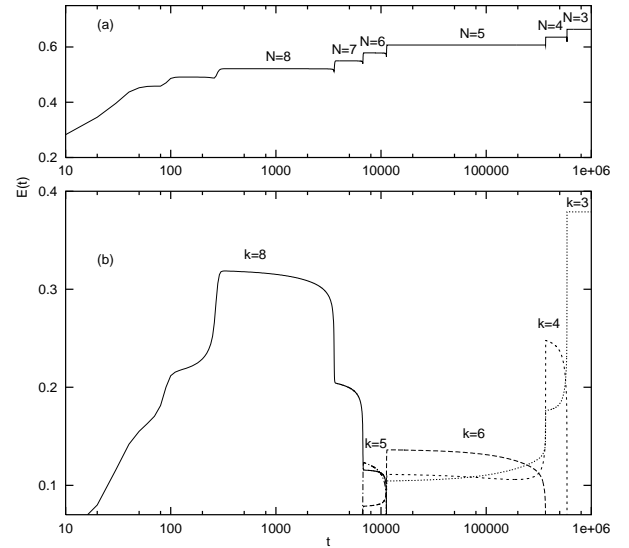


FIG. 1. Simulation of the Cahn–Hilliard equation with  $\beta = 0$ . (a): evolution of the total energy. (b): evolution of the energies of various Fourier modes (as labeled). An inverse cascade is observed from  $N = 8$  to  $N = 3$ . Eventually, the dominant mode becomes  $N = 1$  (not shown in the figure).

We begin with qualitative considerations illustrated by simulations. For  $\beta = 0$ , the solutions to this equation live essentially within a slow manifold of soliton-like solutions with an alternation of plateaus at the zeros  $v = \pm\Gamma$  of the potential, separated by alternating kinks and antikinks [12]. The corresponding fixed points, having  $N$  pairs of regularly spaced kinks and antikinks, are all unstable saddle points of a Lyapunov functional, except for  $N = 1$  which gives a stable absolute minimum. The temporal evolution is a cascade of annihilations of kink-antikink pairs, leading eventually to the gravest  $N = 1$  mode [13]. This is illustrated in Figs. 1 and 2(a) obtained by numerical simulation using the method described in Ref. [7]. In the Fourier space an inverse cascade is observed with

the dominantly excited wavenumber shifting roughly to smaller and smaller wavenumbers (see, e.g. Ref [14] and Fig. 1(b)). Except for the short kink-antikink annihilation episodes, the motion of kinks is described by simple ODE's to be derived below. They involve exponential couplings between adjacent kinks, so that the typical duration of the plateaus increases exponentially as  $N$  decreases.

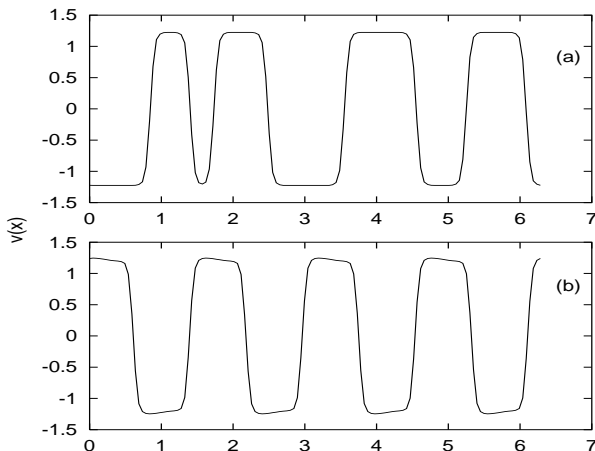


FIG. 2. Solutions with four kink-antikink pairs. (a): snapshot of velocity  $v(x,t)$  in a slowly evolving state for  $\beta = 0$ ; (b): final stable asymptotic state for  $\beta = 10^{-3}$  with  $N = 4$  exhibiting distorted plateaus between the kinks (this is actually a traveling wave measured in a suitable moving frame).

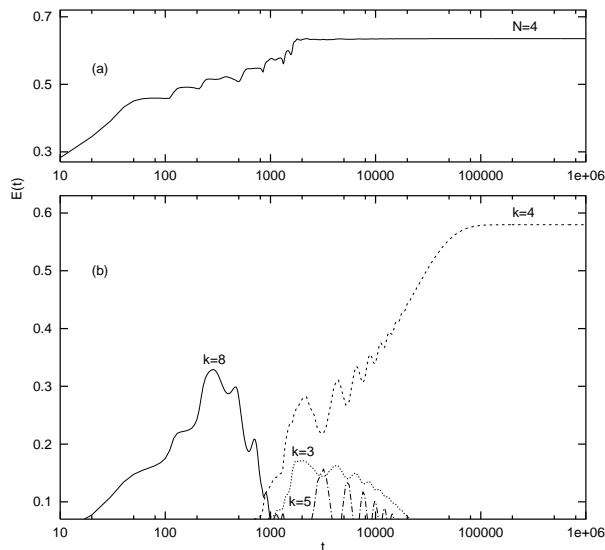


FIG. 3. Same as Fig. 1 but for  $\beta = 10^{-3}$ . Propagating Rossby waves accelerate the cascade and, eventually, halt it when it reaches  $N = 4$  (four pairs of kink-antikinks).

For  $\beta \neq 0$ , the dispersive action of the waves modifies the cascade. For small values of  $\beta$ , the solution retains the characters of kink dynamics with superimposed propagating waves which are expected to predom-

inantly modify the dynamics at large scales where the Rossby wave period is the smallest. As the destabilizing coupling between the kinks decreases exponentially with the typical separation of adjacent kinks, the stabilizing effect of dispersive waves can dominate for solutions of sufficiently large wavelength, thereby halting the inverse cascade at an intermediate wavelength  $\Lambda = L/N$  with integer  $N > 1$ . This is illustrated with a simulation for  $\beta = 10^{-3}$  shown in Fig. 3, where the cascade is found to halt at wavenumber  $k = 4$ , corresponding to a wavelength  $\Lambda = L/4$ .

We turn now to more systematic theory, beginning again with  $\beta = 0$ , case for which we mostly follow Kawasaki and Ohta [10]. The (pure) Cahn–Hilliard equation admits  $M(x) = \pm \Gamma \tanh sx$  as stationary solutions of  $\partial_x^2 M_j - U'(M_j) = 0$ . When the typical separation between kinks is large, a solution with  $N$  kink-antikink pairs may be written, near the  $j$ th kink, as  $v(x,t) = M_j(x) + \tilde{v}_j(x,t)$ , where  $M_j(x) = \epsilon_j M(x - x_j)$  with  $\epsilon_j = (-1)^j$  and exponentially small remainder  $\tilde{v}_j(x,t)$ . Hence, the time derivative is, up to exponentially small terms,  $\partial_t v(x,t) = -\sum_{\ell=0}^{2N-1} \dot{x}_\ell(t) \partial_x M_\ell(x)$ . Substituting into (1), integrating twice in space, multiplying by  $\partial_x M_j$  and integrating over the periodicity interval  $[0, L]$ , we obtain

$$\frac{1}{\lambda_3} \sum_{\ell=0}^{2N-1} \dot{x}_\ell \int_0^L \int_0^L \partial_x M_j(x) \mathcal{G}_2(x-x') \partial_x M_\ell(x') dx dx' = \int_0^L \frac{2s^2}{\Gamma^2} \tilde{v}_j^2 (3M_j + \tilde{v}_j) \partial_x M_j dx - 2\epsilon_j \Gamma h(t), \quad (2)$$

where  $h(t)$  is a time-dependent integration constant which can be determined by the constraint of momentum conservation. Carrying out the integrations in (2), we obtain the ODE's for kink motion:

$$\mathcal{A}_{j\ell} \dot{x}_\ell = e^{-s(x_j - x_{j-1})} - e^{-s(x_{j+1} - x_j)}. \quad (3)$$

Here,  $x_j$  is the location of the  $j$ -th kink and  $\mathcal{A}_{j\ell}$  is a symmetric matrix given by

$$\mathcal{A}_{j\ell} = \frac{1}{8\lambda_3 s^2} \left( \epsilon_{j-\ell} \left( \mathcal{G}_2(x_j - x_\ell) + \frac{\pi^2}{12Ls^2} \right) - \frac{1}{2s} \delta_{j-\ell} \right),$$

where  $\mathcal{G}_2(x)$  is the  $L$ -periodic Green's function satisfying  $\partial_x^2 \mathcal{G}_2(x) = -\delta(x)$ . When  $L \rightarrow \infty$ ,  $\mathcal{G}_2(x_j - x_\ell)$  reduces to  $-|x_j - x_\ell|/2$  and  $\mathcal{A}$  is easily inverted [13]. Although the dynamics described by (3) borrows most of its character from the heteroclinic connection between unstable fixed points, the trajectory in phase-space does not generally proceed from the vicinity of one fixed point to another. Fast jumps from one slow manifold to the next may occur at distance from the fixed points. Thus, as the number of kinks and antikinks decreases with time, the dominating wavenumber does not necessarily decrease monotonically as happens in the ‘‘arithmetic’’ inverse cascade of

Ref. [14]. This may be seen in Fig. 1(b) where the dominant mode goes from wavenumber  $k = 8$ , to 5 and then to 6.

The stability of a given fixed point  $\bar{v}^{(0)}$  of (1) with respect to kink motion is obtained by differentiating (3). It is convenient to define the Fourier components  $\psi_m$  of kink displacements  $\delta x_j$  as  $\psi_m = (2N)^{-1} \sum_{m=0}^{2N-1} \delta x_j e^{-i\pi(mj/N)}$ . After some algebra, we obtain  $\dot{\psi}_m = \sigma_0 \psi_m$  for  $m < N$ , with the eigenvalue  $\sigma_0$  given by

$$\sigma_0 = \frac{128s^3 \lambda_3 e^{-s\Lambda}}{\Lambda} \sin^2 \theta_m \left( 1 - \frac{2(1 - \cos \theta_m)}{s\Lambda} \right)^{-1}, \quad (4)$$

with  $\theta_m = \pi m/N$  and  $\Lambda = L/N$  (the subscript 0 refers to  $\beta = 0$ ). The corresponding eigenvectors for a given  $m$  are  $v_a(x) = \sum_{j=0}^{2N-1} (-1)^j \cos j\theta_m \partial_x M(x - x_j)$  and  $v_b(x) = \sum_{j=0}^{2N-1} (-1)^j \sin j\theta_m \partial_x M(x - x_j)$ . The leading order of (4) corrects a factor 2 error in Ref. [10] in which the exponential variation of  $\tilde{v}_j$  near  $x_{j+1}$  and  $x_{j-1}$  was neglected. Note that our result is consistent with Ref. [15] and agrees with our simulations. For large  $\Lambda$ , all the eigenvalues  $\sigma_0$  (actually  $\sigma_0(m)$ ) for  $m > 0$  are positive, thereby demonstrating the instability of multi-kink-pair solutions.

We now turn to the case of non-vanishing small  $\beta$ , which is studied by a singular perturbation method that we outline. The stationary solution goes over into a (slowly) traveling wave solution which, in a suitable frame moving with the velocity  $c = \beta c_1 + \beta^2 c_2 + O(\beta^3)$ , may be written in the time-independent form  $\bar{v} = \bar{v}^{(0)} + \beta \bar{v}^{(1)} + \beta^2 \bar{v}^{(2)} + O(\beta^3)$ . Here,  $\bar{v}^{(1)}$  and  $\bar{v}^{(2)}$  satisfy  $\mathcal{F}\bar{v}^{(1)} = Q^{(0)}$  and  $\mathcal{F}\bar{v}^{(2)} = Q^{(1)}$  with  $\mathcal{F} \equiv \partial_x^2 - U''$ ,

$$Q^{(0)} \equiv \lambda_3^{-1} \left( c_1 \partial_x^{-1} \bar{v}^{(0)} - \partial_x^{-3} \bar{v}^{(0)} \right), \quad \text{and} \quad Q^{(1)} \equiv \lambda_3^{-1} \left( c_1 \partial_x^{-1} \bar{v}^{(1)} - \partial_x^{-3} \bar{v}^{(1)} + c_2 \partial_x^{-1} \bar{v}^{(0)} \right) + \frac{1}{2} U_0''' \left( \bar{v}^{(1)} \right)^2,$$

where  $U_0 \equiv U(\bar{v}^{(0)})$ . At first order,  $c_1$  is obtained from the solvability condition  $\int_0^L Q^{(0)} \partial_x \bar{v}^{(0)} dx = 0$  as

$$c_1 = - \left( \frac{\Lambda^2}{48} - \frac{\pi^2}{12s^2} + \frac{A}{\Lambda s^3} \right) \left( 1 - \frac{4}{\Lambda s} \right)^{-1}, \quad (5)$$

where  $A = 2.404113 \dots$ . Like  $\sigma_0$  in (4),  $c_1$  is given in (5) up to exponentially small terms (for large  $\Lambda = L/N$ ) and has excellent agreement with numerical simulations. (Note that, at next order,  $c_2$  vanishes.) The first-order perturbation  $\bar{v}^{(1)}$  of the traveling wave profile can also be obtained perturbatively in a large- $\Lambda$  expansion (not given here). This leads to a distorsion of the plateaus, as seen in Fig. 2(b).

The equation governing the perturbation  $\delta v(x, t) \equiv v(x + ct, t) - \bar{v}(x)$  can be written as

$$\begin{aligned} \partial_t \varphi &= \mathcal{L} \varphi, & \varphi &\equiv \partial_x^{-1} \delta v, \\ \mathcal{L} &\equiv -\lambda_3 \partial_x (\partial_x^2 - U''(\bar{v})) \partial_x + c \partial_x - \beta \partial_x^{-1}. \end{aligned} \quad (6)$$

Unlike the case with  $\beta = 0$ , the perturbation to the stationary solution of the  $\beta$ -CH equation does not reduce simply to a change in the kink locations. We must also consider the dispersive effect of the  $\beta$ -term which modifies the shape of the slow modes and contributes to stability. Substitution in (6) of the expansions of  $c$  and  $\bar{v}$  in powers of  $\beta$  leads to an expansion  $\mathcal{L} = \mathcal{L}_0 + \beta \mathcal{L}_1 + \beta^2 \mathcal{L}_2 + O(\beta^3)$ . The unperturbed eigenvalue  $\sigma_0$  becomes  $\sigma = \sigma_0 + i\beta \mu_1 + \beta^2 \sigma_2 + i\beta^2 \mu_2 + O(\beta^3)$ . Similarly, the eigenfunctions  $\varphi_a = \partial_x^{-1} v_a$  and  $\varphi_b = \partial_x^{-1} v_b$  are respectively modified as  $\varphi_a + \beta \varphi_{a1} + \beta^2 \varphi_{a2} + O(\beta^3)$  and  $\varphi_b + \beta \varphi_{b1} + \beta^2 \varphi_{b2} + O(\beta^3)$ . A hierarchy of equations is then obtained for  $\varphi_a, \varphi_b, \varphi_{a1}, \varphi_{b1}, \varphi_{a2}, \dots$ . As is usual in such singular perturbation problems, the corrections to the eigenvalues are obtained from solvability conditions. This gives (with  $\langle f, g \rangle \equiv L^{-1} \int_0^L f g dx$ )

$$\begin{aligned} \langle \varphi_b, \mathcal{L}_1 \varphi_a \rangle &= -\mu_1 \langle \varphi_b, \varphi_b \rangle, \\ \langle \varphi_a, \mathcal{L}_1 \varphi_{a1} \rangle + \langle \varphi_a, \mathcal{L}_2 \varphi_a \rangle &= \sigma_2 \langle \varphi_a, \varphi_a \rangle - \mu_1 \langle \varphi_a, \varphi_{b1} \rangle. \end{aligned} \quad (7)$$

The coefficient  $\mu_1$  gives only the shift in the imaginary part of the eigenvalue. For the real part, the second-order term  $\sigma_2$  is needed. It is obtained from (7); limiting ourselves to leading order large- $\Lambda$  contributions, we obtain after considerable algebra

$$\sigma_2 = - \frac{\Lambda^4}{69,120 s^2 \lambda_3} \frac{q^2 (4 + 9q^2)}{(1 + q^2)^2} + O(\Lambda^3), \quad (8)$$

$$q \equiv \tan \frac{\pi m}{2N}. \quad (9)$$

Note that the correction is negative and, hence, *stabilizing*. Though the effect is small, it increases algebraically with  $\Lambda$ , while the nonlinear coupling of kinks decreases exponentially in (4). Therefore, stabilization of the  $m$ -mode perturbation to the stationary solution is obtained at leading order for large  $\Lambda$  when  $\sigma_0 + \sigma_2 \beta^2 < 0$ , that is

$$|\beta| > \beta_c = \sqrt{35,389,440 \frac{e^{-s\Lambda}}{\Lambda^5} s^5 \lambda_3^2 \frac{1}{4 + 9q^2}}, \quad (10)$$

The condition is the most restrictive for  $m = 1$ , that is  $q = \tan \pi/(2N)$ .

When  $\Lambda$  is only moderately large, an accurate estimate of  $\beta_c$  requires, in principle, a careful determination of  $\varphi_{b1}$  and  $\varphi_{a1}$  by matching of solutions near to and away from the kinks. We have used an alternative semi-numerical approach, which works for all values of  $\Lambda$ , in which the auxiliary equations stemming from the perturbation theory, are solved numerically with a discretization over a quarter-wavelength of  $\varphi_a$  and  $\varphi_b$ , using a procedure written with *Mathematica*, available from the first author (BL). The eigenvalues are obtained from the solvability conditions of the discretized problem, where degeneracies are lifted by imposing symmetries with appropriate boundary conditions for each linear problem to

be solved. We have also solved directly the stability problem by differentiating a Galerkin-truncated expansion of (1) in Fourier modes. Newton's algorithm is used to obtain the traveling solution and its phase velocity; eigenmodes being then calculated with a QR algorithm. The latter procedure provides both the fast and slow modes with exponential separation of the eigenvalues. As the problem becomes very stiff when  $L$  is large, we are in practice limited to values of  $L$  less than a few hundreds.

Table I compares the asymptotic and the semi-numerical solutions of the perturbation theory with the direct solution of the stability problem. There is excellent agreement between the direct calculation and the semi-numerical solution of the perturbation problem for  $N < 5$ . It breaks down when the approximation of separated kinks is no longer valid. The asymptotic result (10) provides then the correct order of magnitude but is wrong by a factor 2 or 3. The convergence to the numerical solution is observed at larger  $L$  but is very slow: multiplying  $L$  by 10 and 50 narrows the discrepancy for mode 2 to 4.6% and 1.3%, respectively.

Numerical temporal integrations of (1) starting from random initial conditions eventually achieves a traveling wave solution with one of the values of  $N$  found stable by the perturbation theory. However, when  $\beta$  is too small it is difficult to achieve a value of  $N$  other than unity, probably because the basin of attraction of other stable solutions does not span a large fraction of the slow manifold. Note that the acceleration of the cascade with respect to the case  $\beta = 0$  is due to the stronger coupling between the kinks provided by the Rossby waves but cannot be quantitatively explained by the perturbation theory near the fixed points.

The main result of our perturbation theory is (10) which gives the minimum value of  $|\beta|$  able to stabilize a solution of period  $\Lambda = L/N$  with  $N > 1$ . By inverting  $\Lambda$  in terms of  $\beta$ , we can explain the halting of the inverse cascade at a wavelength  $\Lambda$  which scales as  $\Lambda = -(2/s) \ln |\beta|$  (to leading order).

N	direct calculation		perturbation (semi-numerical)	perturbation (large $\Lambda$ -asymptotics)	
	$c_1$	$\beta_c$	$\beta_c$	$c_1$	$\beta_c$
2	-35.002	$2.358 \cdot 10^{-6}$	$2.358 \cdot 10^{-6}$	-35.002	$1.45 \cdot 10^{-6}$
3	-16.067	$4.965 \cdot 10^{-4}$	$4.966 \cdot 10^{-4}$	-16.067	$2.20 \cdot 10^{-4}$
4	-9.2073	$1.069 \cdot 10^{-2}$	$1.067 \cdot 10^{-2}$	-9.2090	$3.2 \cdot 10^{-3}$
5	-5.9507	$8.96 \cdot 10^{-2}$	$10.28 \cdot 10^{-2}$	-5.9637	$1.8 \cdot 10^{-2}$

TABLE I. Comparison of the perturbation theory in both its asymptotic and numerical form with the direct stability calculation. The calculation is done for  $L = 76.93$  (10 unstable modes when  $\beta = 0$ ) and several values of  $N$ .

Note that standard phenomenology, based on dimensional analysis à la Rhines [1] with equilibration of nonlinear and Rossby characteristic times, gives a drastically different scaling, namely  $\Lambda \sim |\beta|^{-3}$ . (The nonlinear time is  $\propto \Lambda^2$  and the Rossby time to  $1/(\beta\Lambda)$ ; velocities are  $O(1)$ .) The discrepancy arises, of course, from the failure of dimensional analysis to capture the almost complete suppression of nonlinearity obtained in the plateaus. The latter play here the role of coherent structures in Navier-Stokes turbulence. It would be of interest to study dispersive stabilization for a strongly nonlinear high-Reynolds number inverse cascade of the kind considered by Kraichnan [16]. So far no systematic theory can handle this, although some progress has been made recently on a related passive scalar problem [17].

Finally, we mention that in recent work, devoted to zonal jets in planetary flow, Manfroi and Young [18] studied a closely related problem in which stabilization is provided by a friction term  $-rv$  added to the right hand side of (1). We find that a suitable adaptation of the analysis for the dispersive case gives stabilization for  $r > r_c \sim e^{-s\Lambda}/\Lambda$ .

We are grateful to Joanne Deval for careful checking of all the calculations.

---

\* E-mail: legras@lmd.ens.fr

- [1] P. Rhines, J. Fluid Mech. **69**, 417 (1975).
- [2] R. Panetta, J. Atmos. Sci. **50**, 2073 (1993).
- [3] G. Vallis and M. Maltrud, J. Phys. Ocean. **23**, 1346 (1993).
- [4] T. Nozawa and S. Yoden, Phys. Fluids **9**, 2081 (1997).
- [5] H.-P. Huang and W. A. Robinson, J. Atmos. Sci. **55**, 611 (1998).
- [6] V.E. Zakharov, V.S L'vov and G. Falkovich, *Kolmogorov Spectra of Turbulence I*, Springer (1992).
- [7] U. Frisch, B. Legras, and B. Villone, Physica D **94**, 36 (1996).
- [8] U. Frisch, *Turbulence. The Legacy of A.N. Kolmogorov*, Cambridge University Press (1995).
- [9] L.D. Meshalkin and Ya.G. Sinai, Appl. Math. Mech. **25**, 1700 (1961).
- [10] K. Kawasaki and T. Ohta, Physica **116A**, 573 (1982).
- [11] A.A. Nepomnyashchy, Appl. Math. Mech. **40**, 886 (1976).
- [12] P. W. Bates and J. Xun, J. Diff. Eq. **117**, 165 (1995).
- [13] T. Kawakatsu and T. Munakata, Prog. Theor. Phys. **74**, 11 (1985).
- [14] Z. S. She, Phys. Lett. A **124**, 161 (1987).
- [15] J.S. Langer, Ann. Phys., **65**, 53 (1971).
- [16] R.H. Kraichnan, Phys. Fluids, **10**, 1417 (1967).
- [17] K. Gawędzki and M. Vergassola, Phase transition in the passive scalar advection, preprint cond-mat/9811399 (1998).
- [18] A. Manfroi and W. Young, Slow evolution of zonal jets on the beta-plane, to appear in J. Atmos. Sci. (1998).